Article

Effects of Methyl Substitution on Radiative and Solvent Quenching Rate Constants of [Ru(phen)dppz]$^{2+}$ in Polyol Solvents and Bound to DNA

Johan Olofsson, L. Marcus Wilhelmsson, and Per Lincoln

J. Am. Chem. Soc., **2004**, 126 (47), 15458-15465• DOI: 10.1021/ja047166a • Publication Date (Web): 09 November 2004

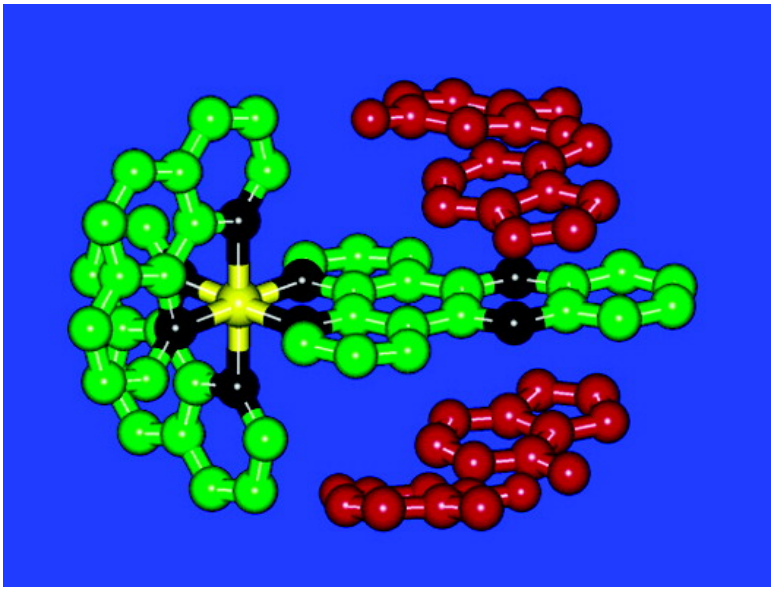

J|A|C|S
ARTICLES
Published on Web 11/09/2004

Effects of Methyl Substitution on Radiative and Solvent Quenching Rate Constants of $[Ru(phen)_2dppz]^{2+}$ in Polyol Solvents and Bound to DNA

Johan Olofsson, L. Marcus Wilhelmsson, and Per Lincoln*

Contribution from the Department of Chemistry and Bioscience, Chalmers University of Technology, S-412 96 Gothenburg, Sweden

Received May 14, 2004; E-mail: lincoln@chembio.chalmers.se

Abstract: Methyl substituents on the distant benzene ring of the dppz ligand in the "light switch" complex $[Ru(phen)_2dppz]^{2+}$ have profound effects on the photophysics of the complexes in water as well as in the polyol solvents ethylene glycol, glycerol, and 1,2- and 1,3-propanediol. Whereas 11,12-dimethyl substitution decreases the rate of quenching by diminishing hydrogen bonding by solvent, the 10-methyl substituent in addition also decreases both the radiative and the nonradiative rate constant for decay to the ground state of the non-hydrogen-bonded excited state species. For both the 10-methyl and the 11,12-dimethyl derivatives, the effect of methyl substitution on the equilibrium of solvent hydrogen bonding to the excited state is due to changes in the entropy terms, rather than in the enthalpy, indicating that the effect is a steric perturbation of the solvent cage around the molecule. When intercalated into DNA, the effects of methyl substitution is smaller than those in polyol solvent or water, suggesting that the water molecules that quench the excited state by hydrogen bonding to the phenazine aza nitrogens mainly access them from the same groove as in which the Ru(II) ion resides. Since the Δ-enantiomer of $[Ru(phen)_2$10-methyl-$dppz]^{2+}$ has an absolute quantum yield of up to 0.23 when bound to DNA, a value 7000 times higher than in pure water solution, it is promising as a new luminescent DNA probe.

Introduction

There are interesting potentials for the use of Ru(II) complexes with 2,2′-bipyridine-type ligands as anticancer drugs, for development of DNA conformational probes, or as photoactivated electron donors for initiation of electron-transfer processes.[1−18] Complexes with an extended planar ligand like dipyrido-[3,2-a:2′,3′-c]phenazine (dppz) are known to intercalate between the base pairs in DNA.[11,17,19−22] The dppz moiety of, e.g., $[Ru(phen)_2dppz]^{2+}$ (phen = 1,10-phenanthroline) is thereby partly protected from the solvent water molecules by the DNA resulting in an enormous increase in quantum yield, the "light switch" effect.[11,19,22−26]

After photoexcitation with visible light, an electron, formally originating from a d orbital in the ruthenium ion, is transferred to an antibonding π^* orbital on the dppz ligand, and a long-lived state of triplet character is formed (metal-to-ligand charge transfer, MLCT).[21,24,25,27−32] The efficient quenching of Ru-dppz complexes in water is proposed to be due to fast hydrogen bonding of solvent to the phenazine aza nitrogens of the dppz anion radical, which are moderately basic due to their partial negative charge, whereas formation of hydrogen bonds to the

(1) Lincoln, B.; Broo, A.; Nordén, B. *J. Am. Chem. Soc.* **1996**, *118*, 2644.
(2) Erkkila, K. E.; Odom, D. T.; Barton, J. K. *Chem. Rev.* **1999**, *99*, 2777.
(3) Nordén, B.; Lincoln, P.; Åkerman, B.; Tuite, E. In *Metal Ions in Biological Systems*; Siegel, A., Siegel, H., Eds.; Dekker, M.: New York, 1996; Vol. 33, p 177.
(4) Haq, I.; Lincoln, P.; Suh, D.; Nordén, B.; Chowdhry, B. Z.; Chaires, J. B. *J. Am. Chem. Soc.* **1995**, *117*, 4788.
(5) Choi, S. D.; Kim, M. S.; Kim, S. K.; Lincoln, P.; Tuite, E.; Nordén, B. *Biochemistry* **1997**, *36*, 214.
(6) Holmlin, R. E.; Stemp, E. D. A.; Barton, J. K. *Inorg. Chem.* **1998**, *37*, 29.
(7) Tuite, E.; Lincoln, P.; Nordén, B. *J. Am. Chem. Soc.* **1997**, *119*, 239.
(8) Dupureur, C. M.; Barton, J. K. *J. Am. Chem. Soc.* **1994**, *116*, 10286.
(9) Dupureur, C. M.; Barton, J. K. *Inorg. Chem.* **1997**, *36*, 33.
(10) Hartshorn, R. M.; Barton, J. K. *J. Am. Chem. Soc.* **1992**, *114*, 5919.
(11) Jenkins, Y.; Friedman, A. E.; Turro, N. J.; Barton, J. K. *Biochemistry* **1992**, *31*, 10809.
(12) Friedman, A. E.; Kumar, C. V.; Turro, N. J.; Barton, J. K. *Nucleic Acids Res.* **1991**, *19*, 2595.
(13) Lincoln, B.; Nordén, B. *Chem. Commun.* **1996**, *18*, 2145.
(14) Önfelt, B.; Lincoln, P.; Nordén, B. *J. Am. Chem. Soc.* **2001**, *123*, 3630.
(15) Önfelt, B.; Göstring, L.; Lincoln, P.; Nordén, B.; Önfelt, A. *Mutagenesis* **2002**, *17*, 317.
(16) Önfelt, B.; Lincoln, P.; Nordén, B. *J. Am. Chem. Soc.* **1999**, *121*, 10846.
(17) Hiort, C.; Lincoln, P.; Nordén, B. *J. Am. Chem. Soc.* **1993**, *115*, 3448.
(18) Wilhelmsson, L. M.; Westerlund, F.; Lincoln, P.; Nordén, B. *J. Am. Chem. Soc.* **2002**, *124*, 12092.
(19) Coates, C. G.; Jacquet, L.; McGarvey, J. J.; Bell, S. E. J.; Al-Obaidi, A. H. R.; Kelly, J. M. *J. Am. Chem. Soc.* **1997**, *119*, 7130.
(20) McGarvey, J. J.; Callaghan, P.; Coates, C. G.; Schoonover, J. R.; Kelley, J. M.; Jacquet, L.; Gordon, K. C. *J. Phys. Chem. B* **1998**, *102*, 5941.
(21) Chen, P. Y.; Meyer, T. J. *Chem. Rev.* **1998**, *98*, 1439.
(22) Coates, C. G.; Olofsson, J.; Coletti, M.; McGarvey, J. J.; Önfelt, B.; Lincoln, P.; Nordén, B.; Tuite, E.; Matousek, P.; Parker, A. W. *J. Phys. Chem. B* **2001**, *105*, 12653.
(23) Olofsson, J.; Önfelt, B.; Lincoln, B.; Nordén, B.; Matousek, P.; Parker, A. W.; Tuite, E. *J. Inorg. Biochem.* **2002**, *91*, 286.
(24) Chambron, J.-C.; Sauvage, J.-P.; Amouyal, E.; Koffi, P. *Nouv. J. Chim.* **1985**, *9*, 527.
(25) Amouyal, E.; Homsi, A.; Chambron, J.-C.; Sauvage, J.-P. *J. Chem. Soc., Dalton Trans.* **1990**, *6*, 1841.
(26) Olson, E. J. C.; Hu, D.; Hörmann, A.; Jonkman, A. M.; Arkin, M. R.; Stemp, E. D. A.; Barton, J. K.; Barbara, P. F. *J. Am. Chem. Soc.* **1997**, *119*, 11458.
(27) Kober, E. M.; Sullivan, B. P.; Meyer, T. J. *Inorg. Chem.* **1984**, *23*, 2098.
(28) Kober, E. M.; Meyer, T. J. *Inorg. Chem.* **1982**, *21*, 3967.
(29) Schoonover, J. R.; Bates, W. D.; Meyer, T. J. *Inorg. Chem.* **1995**, *34*, 6421.
(30) Schoonover, J. R.; Strouse, G. F. *Chem. Rev.* **1998**, *98*, 1335.
(31) Coates, C. G.; Callaghan, P.; McGarvey, J. J.; Kelley, J. M.; Kruger, P. E.; Higgins, M. E. *J. Raman Spectrosc.* **2000**, *31*, 283.
(32) Krausz, E.; Ferguson, J. *Prog. Inorg. Chem.* **1989**, *37*, 293−390.

10.1021/ja047166a CCC: $27.50

Scheme 1. Structures of Ruthenium Complexes

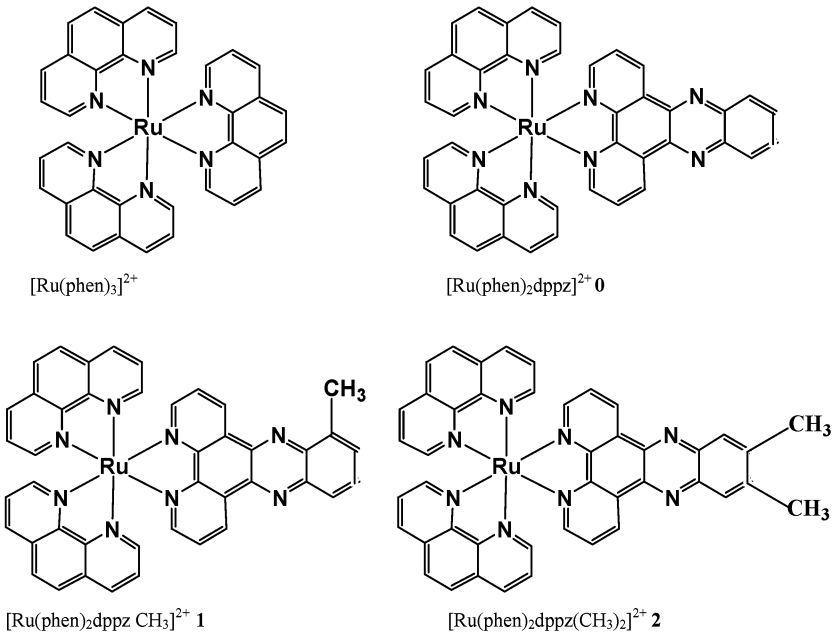

$[Ru(phen)_3]^{2+}$ $[Ru(phen)_2dppz]^{2+}$ **0**

$[Ru(phen)_2dppz\ CH_3]^{2+}$ **1** $[Ru(phen)_2dppz(CH_3)_2]^{2+}$ **2**

ground state does not occur because of the very weak basicity of the Ru^{2+} coordinated, neutral dppz ligand.[24,25,29,33−35] A very short-lived intermediate MLCT state has been detected in water and is suggested to be similar to the non-hydrogen-bonded dppz-localized state which dominates the emission in DNA and in acetonitrile,[26] a conclusion that is supported also by time-resolved resonance Raman spectroscopy studies (TR^3).[22,23] The Ru-dppz complexes bind strongly to DNA[6,11,26,36−38] but the excited-state lifetime, and consequently the luminescence quantum yield, shows a remarkable sensitivity to both the chirality of the ruthenium center and the nature of the ancillary ligands and the nucleic acid sequence.[23,38]

To explain the structural sensitivity of the "light-switch" effect, we here make an effort to increase the understanding of also finer details of the quenching mechanism of Ru-dppz complexes in a hydroxyl-rich environment. We have recently described the temperature dependence of the emission of [Ru(phen)$_2$dppz]$^{2+}$ in the following hydroxylic solvents: glycerol, ethylene glycol, 1,2- and 1,3-propandiol, ethanol, and water.[39,40] Two types of elementary emission spectral profiles were required to fit all measured emission spectra in the polyol solvents over a large temperature range (10 °C to 150 °C). Emission spectra of the two differently solvated species and their concentration profiles could be deconvoluted from the data. The results showed that a third nonemissive excited-state species has to be involved to explain the experiments. It was suggested that the two emissive species corresponded to MLCT states with zero and one hydrogen-bonded solvent molecule, respectively, and that the nonemissive state corresponded to an excited state where both phenazine nitrogens of the dppz ligand were hydrogen bonded to solvent molecules.

In the present work we extend the earlier study to include complexes modified by methyl substitution on the outermost benzene ring of the dppz ligand (Scheme 1). Inspiration to this study came from the paper by Hartshorn et al.,[10] where a spectacular lengthening of the excited state lifetimes was observed for the racemic 10-methyl dppz complex bound to DNA. The 10-methyl group could be expected to sterically shield the nitrogen in the *peri*-position from hydrogen bonding, thus the reduced rate of quenching observed by Hartshorn et al. seemed to confirm our hypothesis of the necessity of hydrogen bonding to both phenazine nitrogens to completely quench the luminescence of $[Ru(phen)_2dppz]^{2+}$. However, to our surprise, we found that methyl groups also in the more remote 11,12-positions of the dppz decreased the hydrogen bonding of the excited state by solvent, when intercalated not only into DNA but even more pronouncedly in water and several polyols. Thus, methyl groups appear to have an effect that cannot be attributed solely to direct sterical interference with hydrogen bond formation. Furthermore, in the 1,2- and 1,3-propanediol solvents, the enthalpy cost for breaking a hydrogen bond to the excited state was found to be essentially the same for two methylated complexes as for the parent unsubstituted complex.

Our conclusion is that the decreased hydrogen bonding in the methylated complexes is due to an entropic effect, caused by a steric perturbation of the whole solvation cage around the dppz-ligand by the methyl groups. As smaller effects from methyl substitution are found with DNA compared to the polyol solvents, we suggest that when the complexes are intercalated into DNA, water molecules can mainly access the phenazine nitrogens from that side of DNA where the Ru(II) ion is situated and not from the side of the methyl groups.

(33) Chambron, J.-C.; Sauvage, J.-P. *Chem. Phys. Lett.* **1991**, *182*, 603.
(34) Yam, V. W. W.; Lo, K. K.-W.; Cheung, K. K.; Kong, R. Y. C. *Chem. Commun.* **1995**, *11*, 1191.
(35) Nair, R. B.; Cullum, B. M.; Murphy, C. J. *Inorg. Chem.* **1997**, *36*, 962.
(36) Turro, C.; Bossmann, S. H.; Jenkins, Y.; Barton, J. K.; Turro, N. J. *J. Am. Chem. Soc.* **1995**, *117*, 9026.
(37) Sabatani, E.; Nikol, H. D.; Gray, H. B.; Anson, F. C. *J. Am. Chem. Soc.* **1996**, *118*, 1158.
(38) Friedman, A. E.; Chambron, J. C.; Sauvage, J.-P.; Turro, N. J.; Barton, J. K. *J. Am. Chem. Soc.* **1990**, *112*, 4960.
(39) Olofsson, J.; Önfelt, B.; Lincoln, P. *J. Phys. Chem. A* **2004**, *108*, 4391−4398.
(40) Önfelt, B.; Olofsson, J.; Lincoln, P.; Nordén, B. *J. Phys. Chem. A* **2003**, *107*, 1000.

Materials and Methods

Fluorescence Measurements. Steady-state emission measurements were carried out using a Spex fluorolog-3 with the Datamax software. Wavelength of excitation was 440 nm and steady-state emission intensity was measured in the range 450−1000 nm. Absolute quantum yields were obtained by comparing integrated intensities of corrected emission spectra of Ar-purged solutions of the complexes at 25 °C with those of fluorescein in 0.1 M aqueous NaOH as reference (Φ = 0.93).[42] Luminescence measurements were performed in the temperature range 10 °C to 150 °C. Two devices were used to cover the temperature range: a circulating water bath (5 °C to 70 °C) and a cell holder with an electrical heater (20 °C to 200 °C) built in house. Measurements above 150 °C are not included in the study because at higher temperatures irreversible spectral effects begin to appear. For each of **0**, **1**, or **2**, the steady-state emission spectra between 580 and 770 nm, obtained in glycerol, ethylene glycol, and 1,2- and 1,3-propanediol at 10−150 °C, were collected as columns in matrices and subjected to factorization by singular value decomposition (SVD; see Supporting Information).

Transient Emission Measurements. Nanosecond-to-microsecond emission decay measurements were performed on a setup where the exciting light is provided by a pulsed Nd:YAG laser (Continuum Surelite II-10, pulse width < 7 ns) pumping an OPO (optical parametric oscillator) giving a tunable wavelength between 400 and 700 nm. Emitted light is collected at an angle of 90° relative to the excitation light and is sent through a monochromator (symmetrical Czerny-Turner arrangement) and detected by a five-stage Hamamatsu R928 photomultiplier tube. Decays were collected and averaged by a 200 MHz digital oscilloscope (Tektronix TDS2200 2Gs/s) and stored by a LabView program (developed at the department), which controls the whole instrument setup. The oscilloscope is triggered by a signal that is provided by an electronic laser controller.

In the experiments an excitation wavelength of 450 nm was used and emission decays were probed at 600, 650, and 700 nm for the measurements in different solvents and at 610 nm for the measurements in DNA. In general 16 decays were collected and averaged for each sample. The energy of the exciting laser was kept below 20 mJ/pulse to prevent photodegradation of the samples.

Flow Linear Dichroism. Linear dichroism (LD) is defined as the difference in absorbance of linearly polarized light parallel and perpendicular to a macroscopic orientation axis (here the flow direction):[1]

$$\mathrm{LD}(\lambda) = A_{\parallel}(\lambda) - A_{\perp}(\lambda) \quad (1)$$

The reduced linear dichroism LD^{r} is calculated as

$$\mathrm{LD}^{\mathrm{r}}(\lambda) = \mathrm{LD}(\lambda)/A(\lambda)_{\mathrm{iso}} \quad (2)$$

where A_{iso} represents the absorbance of the same isotropic sample. The LD^{r} of a single electronic transition, i, in a flow oriented sample can be written as

$$LD^{\mathrm{r}}_{i} = \frac{3}{2}S(3\cos^2\alpha_i - 1) \quad (3)$$

where α_i is the angle between the transition moment and the molecular orientation axis, in this case, the DNA helix axis, and S denotes the degree of DNA orientation, $0 \leq S \leq 1$. Samples with ruthenium complex and DNA were oriented in a Couette flow cell with an outer rotating cylinder at a shear gradient of 3000 s^{-1}. LD spectra were measured on a Jasco J-720 CD spectropolarimeter equipped with an Oxley prism to obtain linearly polarized light.[1] All spectra were recorded between 220 and 650 nm and baseline-corrected by subtracting the spectrum recorded for the nonoriented sample.

Kinetic Analysis. TCSPC traces were fitted to a sum of exponentials [$S(t) = \Sigma\, \alpha_i \exp(-t/\tau_i)$], using a homemade routine in the framework of the software package Matlab, the first 20 ns being cut off to get rid of the contribution from the lamp pulse (width = 10 ns).

Chemicals. The complexes were synthesized as described elsewhere from the appropriate phenylenediamines,[17] with the exception that the BF_4^- counterion was used for isolation and chromatography rather than the PF_6^-, a procedure that virtually eliminated the last traces of impurities (presumably $[Ru(phen)_3]^{2+}$) that were luminescent in water solution. 2,3-Diaminotoluene and 4,5-diamino-*ortho*-xylene were obtained from Sigma-Aldrich and used as obtained. Glycerol (>99.5%, spectrophotometric grade, water content less than 0.1%), ethylene glycol (>99.8%), 1,2-propandiol (>99.5%), and 1,3-propandiol (>99%) were purchased from Sigma-Aldrich. Argon-purging of the glycerol solution did not change the emission intensity for either $[Ru(phen)_3]^{2+}$ or $[Ru(phen)_2dppz]^{2+}$ in the temperature range 10−150 °C. Poly(dAdT)$_2$ (Pharmacia Biotech) and calf thymus DNA type I (Sigma-Aldrich) were used as received and reconstituted in 10 mM NaCl aqueous solution.

Results

Absorption and Linear Dichroism. Absorption spectra of the metal complexes **0**, **1**, and **2** in 1,2-propanediol (spectra obtained in the different solvents used here were practically superimposable) are shown in Figure 1. As can be observed the methyl substitution on the dppz ligand has a negligible effect on MLCT absorption band at 440 nm; however, the perturbation of the dppz chromophore is significant in the intraligand (IL) $\pi \rightarrow \pi^*$ bands around 375 nm and 300 nm.

Binding of the metal complexes to calf thymus DNA was studied using linear dichroism (LD), and spectra are shown in Figure 2. Flow LD spectra of **0**, **1**, and **2** bound to calf thymus DNA differ significantly only at the position of the IL bands at 375 and 300 nm. In these IL bands, the difference in absorption and LD of the methyl-substituted complexes, obtained by subtracting the spectrum of the parent complex, **1**-**0** and **2**-**0**, have virtually identical shapes (see Supporting Information). The reduced linear dichroism calculated for these difference spectra show that the perturbed transition moments have an effectively perpendicular orientation relative to the helix axis of DNA, perfectly in agreement with the notion that the dominating effect of methyl substitution is a perturbation of the in-plane $\pi \rightarrow \pi^*$ transitions of the dppz ligand. We conclude that the intercalation binding geometries of the enantiomers of **0**, as well as their characteristic effects on the DNA orientation factor, remains identical after methyl substitution.

Quantum Yield and Excited-State Decay in DNA: For all three pairs of enantiomers, the luminescence quantum yields and lifetimes were in general found to be roughly comparable whether intercalated in natural, mixed sequence calf thymus DNA or in the synthetic polymer [poly(dAdT)]$_2$ (Table 1). Thus, when discussing the results we will use the data from the latter, more well-defined system. For all six complexes, the luminescence decay curves had to be fit with two lifetimes. In [poly(dAdT)]$_2$, the lifetimes range almost 2 orders of magnitude, from 3963 ns (Δ-**1**) to 42 ns (Λ-**0**), although the pre-exponential factors show no dramatic variations; for the long lifetime they range from 34% (Λ-**0**) to 69% (Δ-**2**). The ratio of long to short lifetime is remarkably constant with an average of 5.2 (range 4.2−7.4) (Figure 3). Another surprisingly constant ratio is that of the corresponding lifetimes for the Δ- vs the Λ-enantiomer,

(41) Barton, J. K.; Goldberg, J. M.; Kumar, C. V.; Turro, N. J. *J. Am. Chem. Soc.* **1986**, *107*, 2081.
(42) Magde, D.; Wong, R.; Seybold, P. G. *Photochem. Photobiol.* **2002**, *75*, 327.

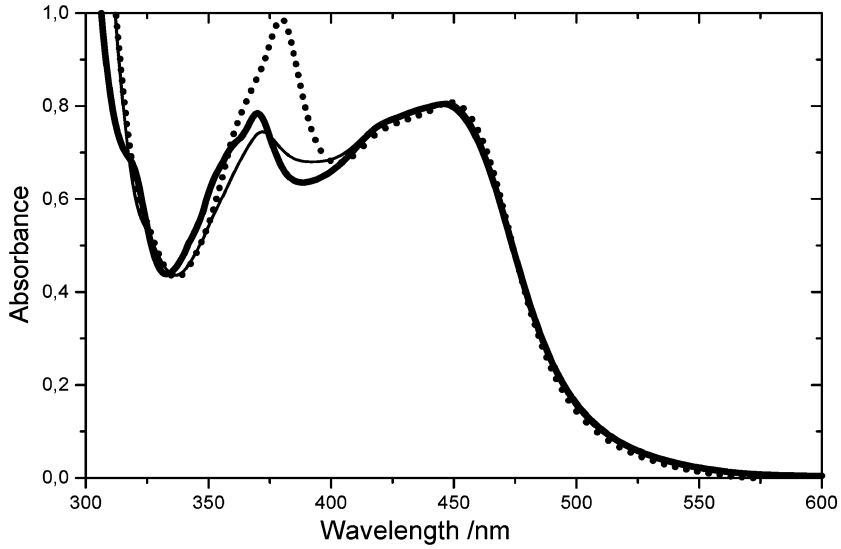

Figure 1. Absorbance of [Ru(phen)$_2$dppz]$^{2+}$ **0** (bold), [Ru(phen)$_2$dppz-CH$_3$]$^{2+}$ **1** (thin), and [Ru(phen)$_2$dppz(CH$_3$)$_2$]$^{2+}$ **2** (dotted) in 1,2-propanediol.

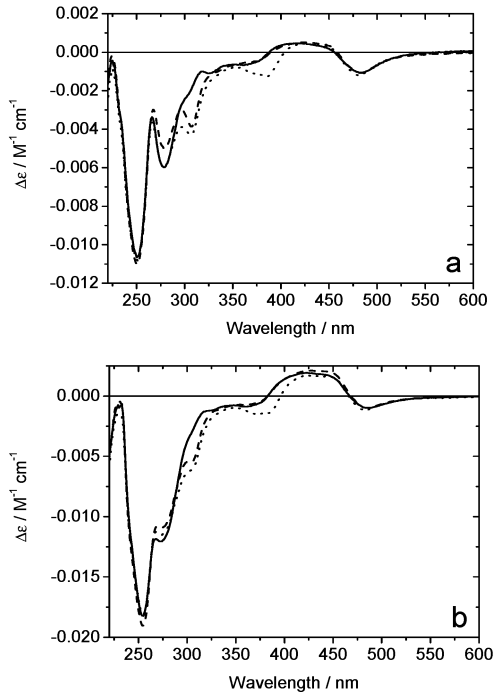

Figure 2. Linear dichroism (LD) spectra of the Δ (panel A) and Λ (panel B) forms of **0** (solid), **1** (dashed), and **2** (dotted) bound to calf thymus DNA. Salt concentration [NaCl] = 10 mM, binding ratio [nucleotide]/[Ru complex] = 10, and concentration of ruthenium complex = 3 μM. Experiments performed at 25 °C.

which has an average of 3.3 (range 2.1−4.2) (Figure 4). The absolute luminescence quantum yields of Δ-**1** and Δ-**2** when bound to DNA are both surprisingly high (20−23%), about 3 times that of Δ-**0**. The high quantum yield and high intensity increase compared to pure water solution (7000 times) should make Δ-**1** a valuable luminescent label for DNA. The differences in quantum yields caused by methyl substitution are even larger for the Λ-enantiomers, the luminescence quantum yields of Λ-**1** being 7 and of Λ-**2** being 4 times higher than that of Λ-**0**. In contrast, the ratio of lifetimes **1** vs **2** is on the average 3.1 (both enantiomers included, range 2.7−3.6), and the ratio of lifetimes **2** vs **0** has an average of 1.6 (range 1.1−1.9). This discrepancy between the lifetimes and the quantum yields shows

Table 1. Photophysical Data for the Δ- and Λ-Enantiomers of **0**, **1**, and **2** Bound to Poly[dAdT]$_2$ (AT) and Calf Thymus DNA (CT)

Ru complex	DNA	Φ[a]/%	τ_1/ns[b] (α/%)	τ_2/ns (α/%)	τ_{NAT}/μs	λ_{em}/nm
Δ-**0**	AT	7.29	774 (59)[c]	134 (41)[c]	7.0	625
Δ-**1**	AT	22.8	3963 (43)	905 (57)	9.7	611
Δ-**2**	AT	19.1	1248 (69)	250 (31)	4.9	616
Λ-**0**	AT	1.37	310 (34)[c]	42 (66)[c]	9.7	625
Λ-**1**	AT	9.85	944 (57)	227 (43)	6.5	622
Λ-**2**	AT	5.52	348 (61)	76 (39)	4.4	620
Δ-**0**	CT	7.01	699 (60)[c]	124 (40)[c]	6.7	622
Δ-**1**	CT	20.17	3091 (62)	587 (38)	10.6	611
Δ-**2**	CT	18.11	1257 (63)	227 (37)	4.8	612
Λ-**0**	CT	0.95	233 (19)[c]	46 (81)[c]	8.6	632
Λ-**1**	CT	9.13	1299 (46)	277 (54)	8.2	618
Λ-**2**	CT	5.43	360 (60)	82 (40)	4.6	617

[a] Absolute quantum yield (Φ) at 25 °C. [b] The wavelength of excitation for the transient emission measurements was 450 nm and the emission wavelength for complex bound to DNA was 610 nm, [base]/[Ru] = 10 and [Ru] = 3 μM at 23 °C. [c] Lifetimes and α-values from Hiort et al..[17]

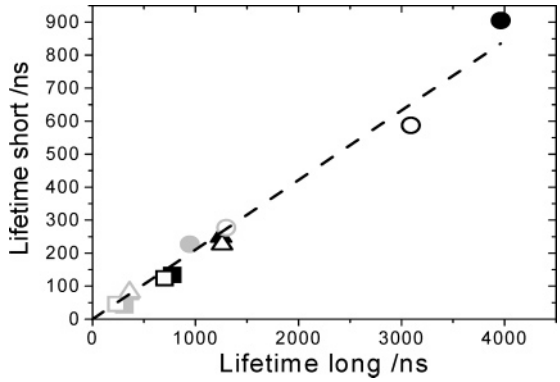

Figure 3. Short against long lifetime of Δ- (black) and Λ- (gray) enantiomers of the following complexes: **0** (square), **1** (circle), and **2** (up triangle) bound to poly[dAdT]$_2$ (filled) and calf thymus DNA (open) are shown. Wavelength of excitation was 450 nm, emission was measured at 610 nm, binding ratio [nucleotide]/[Ru complex] = 10, and salt concentration [NaCl] = 10 mM. Dashed line shows the average ratio τ_{LONG}/τ_{SHORT} = 5.2.

in itself as an unsystematic variation of the apparent natural lifetimes calculated as $\tau_{NAT} = (\alpha_1\tau_1 + \alpha_2\tau_2)/\Phi$ which range from 4.4 to 9.7. An obvious reason for the discrepancies between the natural lifetimes calculated for the polyol solvents and for binding to DNA is the presence of significant proportions of

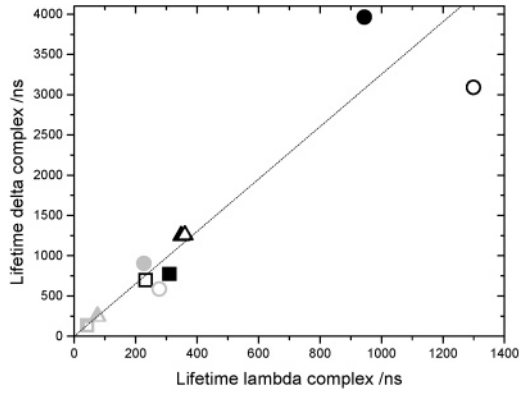

Figure 4. Lifetime for Δ against lifetime of Λ shown for the following ruthenium complexes: **0** (square), **1** (circle), and **2** (up triangle) binding to poly[dAdT]$_2$ (filled symbols) and calf thymus DNA (open symbols). Long lifetimes are marked with black color, and short lifetimes, with gray. Dashed line shows the average ratio lifetime(Δ)/lifetime(Λ) = 3.3.

Table 2. Photophysical Data for **0**, **1**, and **2** in Glycerol (Gly), Ethylene Glycol (Eg), 1,2-propanediol (1,2-pd), 1,3-propanediol (1,3-pd), and Water

Ru complex	solvent	Φ/%	*t*/ns	τ_{NAT}/μs	λ_{em}/nm
0	Gly	0.13	8.2[b]	6.3	639
1	Gly	0.62	53.8	8.7	625
2	Gly	0.56	31.0	5.5	621
0	Eg	0.12	7.5	7.1	656
1	Eg	0.88	71.6	8.1	630
2	Eg	0.68	38.3	5.6	626
0	1,2-pd	1.54	85.7	5.6	619
1	1,2-pd	8.59	941	11.0	617
2	1,2-pd	7.72	454	5.9	611
0	1,3-pd	0.46	27.1	5.9	621
1	1,3-pd	4.00	387	9.7	617
2	1,3-pd	3.40	192	5.6	611
0	H_2O	0.000 93			758
1	H_2O	0.0033			724
2	H_2O	0.023			707

[a] Absolute quantum yield (Φ) at 25 °C. [b] To additional lifetimes of 0.63 ns and 2.3 ns make significant contributions in glycerol at 25 °C.[40]

species with lifetimes short enough to escape detection in the latter case. However, we cannot at present exclude the other possibility being that intercalation into the relatively rigid DNA molecule may also affect the radiative and nonradiative rate constants differently from the polyol solvents.

Quantum Yield, Excited-State Decay and Temperature Variation of Emission Spectra in Polyol Solvents. The quantum yield of **1**, in all four solvents, is slightly higher than that of **2**, the average ratio being 1.2 (range 1.1−1.3); however, the average ratio of lifetimes **1** vs **2** is 2.0 (range 1.9−2.1, glycerol excluded), and the average ratio of lifetimes **2** vs **0** is 5.9 (range 5.1−7.1, glycerol excluded) (Table 2). Thus, the average of the natural lifetime, $\tau_{NAT} = \tau/\Phi$, is significantly longer for **1**, $\langle\tau_{NAT}\rangle = 9.4$ μs (range 8.1−11.0) compared to 5.6 μs (range 5.5−5.9) for **2** and 6.2 μs (range 5.6−7.1) for **0**.

The logarithmic plots of quantum yield against temperature are similar for all three complexes, but the intensity maxima are higher and are shifted toward lower temperatures for **1** and **2** (Figure 5). In fact, the effect of methyl substitution on the log(Φ) vs *T* profile of **0** in ethylene glycol can be compared to that of changing the solvent to 1,3-propanediol. Very interestingly though, all 12 curves still tend to converge to a single line in the high-temperature limit.

Figure 6 shows the steady-state concentration profiles, and

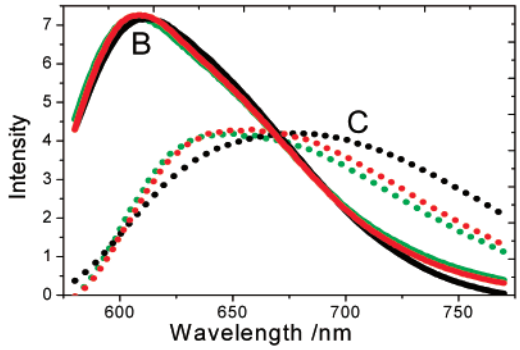

Figure 6. Temperature- and solvent-independent emission spectra of the "B" (solid line) and the "C" (dotted line) species of **0**, **1**, and **2**, determined from deconvolution of the emission spectra in the temperature range 10 °C−150 °C in the four polyol solvents (glycerol, ethylene glycol, and 1,2- and 1,3-propanediol).

Figure 7, the component B and C emission spectra that were

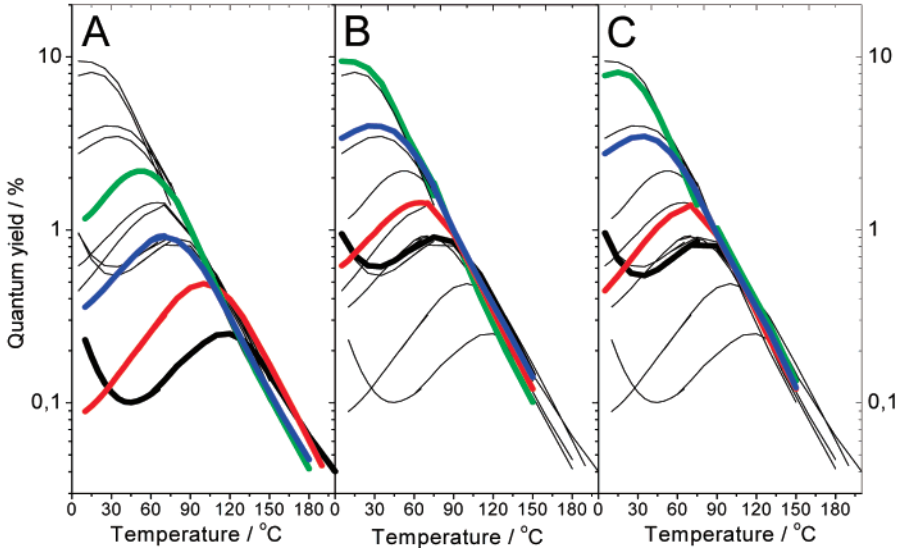

Figure 5. Absolute quantum yield (%) as a function of temperature for **0** (a), **1** (b), and **2** (c) in the following solvents: 1,2-propanediol (green), 1,3-propanediol (blue), ethylene glycol (red), and glycerol (black) (for ease of comparison, all spectra are shown as thin black lines in each figure).

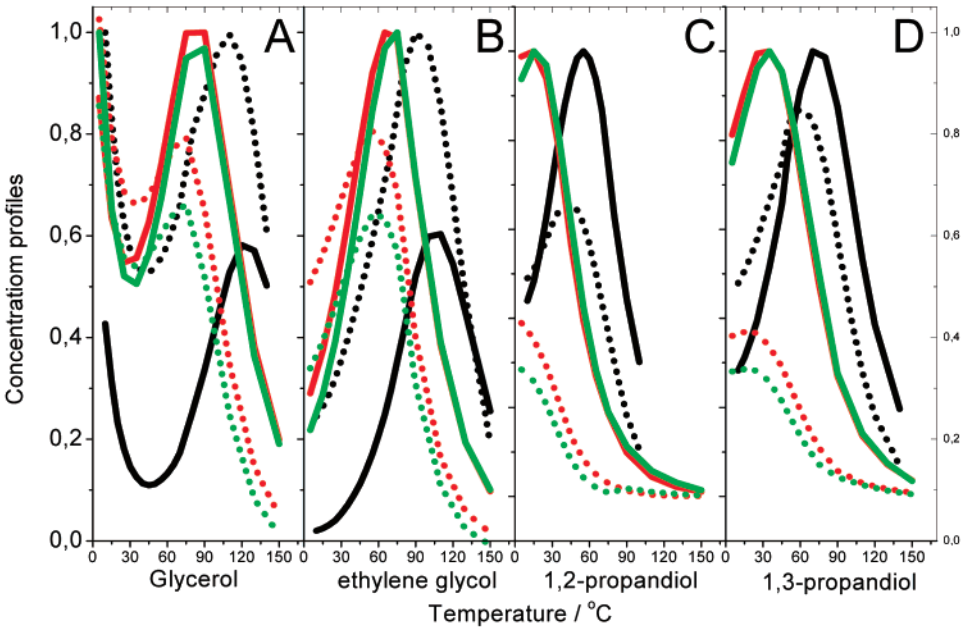

Figure 7. Concentrations of species "B" (solid line) and "C" (dotted line), corresponding to the emission spectra in Figure 6, of **0** (black), **1** (red), and **2** (green) in glycerol (A), ethylene glycol (B), and 1,2- (C) and 1,3-propanediol (D).

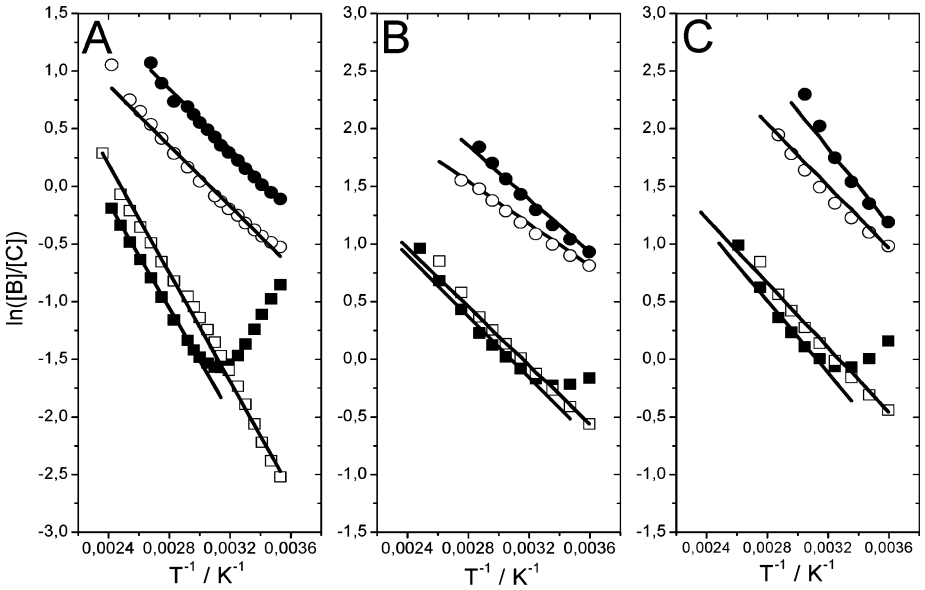

Figure 8. van't Hoff plots of natural logarithm ln([B]/[C]) against inverse temperature T^{-1} for **0** (A), **1** (B), and **2** (C) in glycerol (■), ethylene glycol (□), 1,2-propanediol (●), and 1,3-propanediol (○).

obtained by SVD-aided deconvolution (see Supporting Information) of the steady-state emission spectra for **0**, **1**, and **2** obtained in the polyol solvents at 10−150 °C. Although the criterion of non-negativeness of concentration profiles and component emission spectra was sufficient to provide a unique deconvolution only for **0**,[39] in the case of **1** and **2** we used the deconvolution that gave maximal similarity of the B and C component spectra to the corresponding ones of **0**. Indeed, the emission spectra of the non-hydrogen-bonded B components were then virtually identical for all three complexes, but the spectra of the C component were also very similar. Taken together with the identical MLCT bands in the absorption spectra (Figure 1), this observation suggests that the electronic perturbation of the excited MLCT state energies by methyl substitution is negligible, whether they are hydrogen bonded or not.

As shown in Figure 7, the relative proportion of B compared to C in the steady-state luminescence is much higher for **1** and **2** than compared to **0**. Despite the fact that the calculated concentrations show complicated temperature dependencies, a plot of the logarithm of the ratio between the calculated concentration profiles, ln([B]/[C]), against the inverse of the temperature, $1/T$ (a van't Hoff plot), gave practically linear graphs for **0**, **1**, and **2** in ethylene glycol and 1,2- and 1,3-propanediol and two linear regions in glycerol (Figure 8).

The linearity of the van't Hoff plots strongly supports the notion of a rapid equilibrium between B and C, i.e., that $[B]_{ss} = K_{BC}\,[C]_{ss}$ where

$$\ln K_{BC} = -\frac{\Delta H^{\circ}_{BC}}{RT} + \frac{\Delta S^{\circ}_{BC}}{R} \qquad (4)$$

Table 3. Enthalpy Change for Breaking a Hydrogen Bond to the Metal Complex Calculated from a van't Hoffs Plot (ln[B]/[C] against T^{-1}) in Glycerol (Gly), Ethylene Glycol (Eg), and 1,2- (1,2-pd) and 1,3-Propanediol (1,3-pd)

solvent	$[Ru(phen)_2dppz]^{2+}$ ΔH (kJ mol^{-1})	$[Ru(phen)_2dppzCH_3]^{2+}$ ΔH (kJ mol^{-1})	$[Ru(phen)_2dppz(CH_3)_2]^{2+}$ ΔH (kJ mol^{-1})
Gly	19	11	13
Eg	20	11	12
1,2-pd	11	10	14
1,3-pd	11	11	11

with the enthalpy ($\Delta H°_{BC}$) and the entropy ($\Delta S°_{BC}$) terms being independent of temperature. The enthalpies for the equilibrium between C and B, i.e., the enthalpy change for a solvent molecule to break a hydrogen bond to the excited state, obtained from the slopes of the linear portions of the graphs, are given in Table 3. Very interestingly, the $\Delta H°$ values are little affected by methyl substitution in the propanediol solvents, indicating that the strength of a hydrogen bond to the aza nitrogen of the negatively charged dppz moiety of the excited state remains the same. The increase in the equilibrium constant found for **1** and **2** relative to **0** in these solvents, thus, has to be due to an increase in $\Delta S°$, supporting the notion that the effect of the methyl substitution primarily is sterical rather than electronic. However, the $\Delta H°$ values in ethylene glycol and glycerol, which for **0** are about twice as large as in the propanediols, are almost the same as those in the other two solvents for **1** and **2**, although the equilibrium constants in ethylene glycol and glycerol remain smaller. Since ethylene glycol and glycerol can be expected to form a more dense and structured hydrogen-bonded network around the solute than the propanediols, it seems likely that this solvent structure would increase coupling of enthalpy and entropy changes of solvation.

Quite surprisingly, the emission quantum yield of **2** in pure water at 25 °C is 25 times that of **0** and 7 times that of **1**. Furthermore, **2** shows a slight decrease of emission quantum yield with increasing temperature, in contrast to the two other complexes that show an increase. This anomalously high quantum yield in water for **2**, which with its two methyl groups has the largest hydrophobic area of the three complexes, underscores the importance, for strongly hydrogen-bonded solvents, of the complete solvation shell around the charged dppz ligand in the excited state.

Discussion

Compared to the parent $[Ru(phen)_2dppz]^{2+}$ complex **0**, the homologues **1** and **2** methylated in the distant benzene ring of the dppz ligand show dramatically increased luminescence lifetimes and quantum yields in polyol solvents at room temperature. A qualitatively similar, but less dramatic, effect of methyl substitution on the photophysical properties is found also when the complexes, in their enantiomerically pure forms, are intercalated into DNA in aqueous solution.

In the analysis of these observations, we shall adopt the model previously developed for the parent compound **0** in polyol solvents (Scheme 2).[39] Within the time scale of the present experiments, we encounter first the dppz-localized charge transfer state B which initially is *not* hydrogen bonded by solvent when it is formed from the intermediary state or states represented by A.[40] Consecutive hydrogen bonding from solvent

Scheme 2. Schematic Model of Relaxation Pathways[a]

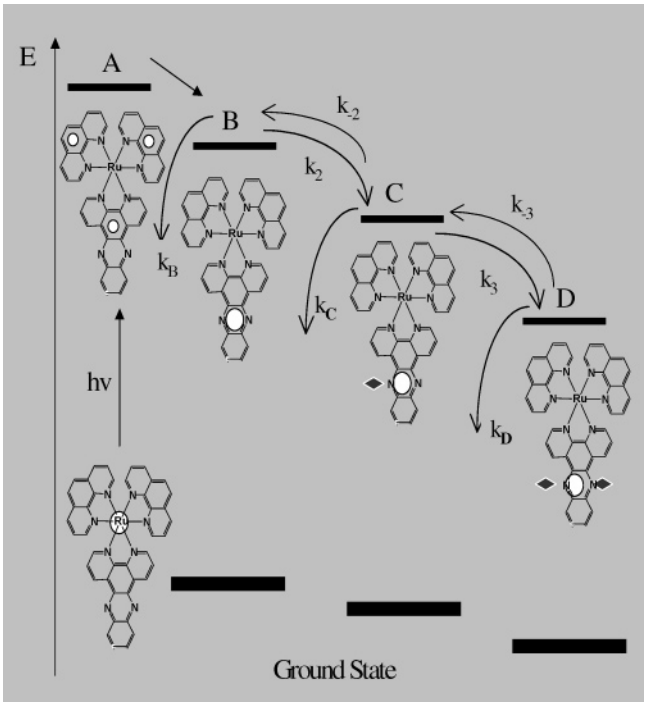

[a] Upon excitation of an electron from a d orbital in ruthenium (ground state), state B (no hydrogen bond), where the electron is localized on the dppz ligand, is rapidly formed from the intermediary state(s) A. State C and D are two subsequently formed excited states which corresponds to one or two solvent molecules (depicted as diamonds) hydrogen bonded to the phenazine nitrogens on the dppz ligand.

to the lone pairs of the two aza nitrogens can form species C and D, in which just one or both of these nitrogens are hydrogen bonded, respectively. Species D was assumed to be nonluminescent, and from a simple kinetic modeling of the time-evolution of the emission profile of **0** in glycerol at 25 °C, species C was estimated to have about a 30% lower quantum yield than B.[40]

Spectroscopic and thermodynamic data suggest that methyl substitution does not primarily affect the enthalpy of hydrogen bond formation from solvent, making it less exothermic, but instead acts by increasing the entropy cost of hydrogen bond formation. Surprisingly, the effect of methyl substitution is almost as pronounced at the more distant 11,12-positions in **2** as in the immediate vicinity of the aza nitrogen in the 10-position in **1**, where it could be imagined to be a direct steric hindrance to hydrogen bond formation, indicating that the whole solvation shell around the charged dppz ligand is of importance.

The difference between **1** and **2** in their photophysical properties in the polyol solvents is mainly in the lifetimes, which are significantly longer for **1**, seemingly confirming the importance of direct sterical hindrance for reducing the rate constant of quenching by hydrogen bonds from solvent. However, since the quantum yields are much more similar, also the radiative rate constant (the inverse of which is the natural lifetime) is decreased in **1** compared to **2**. By contrast, the radiative rate constants appear to be roughly similar in **2** and **0**.

The excited-state lifetime can be approximated as $(k_B + K_I K_{II} k_D)^{-1}$, under the assumptions that state B is the dominating species and that the equilibration of the excited states B, C, and D is much faster than the deactivation processes to the ground state (as evidenced by the linear van't Hoff plots of the

polyol solvents of Figure 8). In this expression, $k_B = k_{BF} + k_{BQ}$ is the sum of the radiative and nonradiative decay rate constants of B, $K_I = k_2/k_{-2}$ and $K_{II} = k_3/k_{-3}$ are the equilibrium constants between B and C or C and D, respectively, and k_D is the, by assumption, nonradiative decay rate constant of D (see Scheme 2). At 25 °C, quantum yields increase with increasing temperature, indicating that k_B (and k_C) is small compared to $K_I K_{II} k_D$ and that the latter actually decreases with increasing temperature due to the exothermicity of hydrogen bond formation. From Figure 8, K_I can be estimated to be very similar for **1** and **2**; however, we cannot tell whether the increase in lifetime for **1** is due to a smaller K_{II} (which would be expected if the 10-methyl group excerted a steric hindrance for formation of the second hydrogen bond) or a smaller k_D. That the latter may in fact be the case is supported by the observation that the lifetime of **1** compared to **2** is still about twice as long in 1,2-propanediol at 80 °C, where k_B now dominates over $K_I K_{II} k_D$ (data not shown), thus not only the radiative rate constant k_{BF} but also the nonradiative rate constant k_{BQ} can be concluded to be smaller in **1** compared to **2**, indicating that we cannot rule out that k_D might as well be sensitive to the position of the methyl substitution on the dppz ligand.

When bound to poly[dAdT]$_2$, the average ratio of comparable excited-state lifetimes for **2** vs **0** is 1.9, which is significantly smaller than the average ratio 5.9 found in the diol solvents (in these solvents the two complexes were found to have very similar natural lifetimes, $\langle \tau_{NAT} \rangle = 5.6$ μs and 6.2 μs for **2** and **0**, respectively). If the water molecules primarily would access the phenazine nitrogens from the groove opposite to the one in which the Ru(II) ion resides in the intercalated DNA binding mode, the effect of the 11,12-dimethyl substitution on the solvation, and hence the water quenching rate, would have been expected to be even more pronounced than in the pure solvents (especially since the luminescence quantum yield of **2** in water is approximately 25 times larger than that of **0**). On the other hand, if the quenching by water mainly takes place from the groove where the Ru(II) ion resides, the rates would be expected to be less affected by the 11,12-dimethyl substitution which is in fact what we observe. However, if the dppz ligand was deeply intercalated, with the phenazine nitrogens at the center of the base pair in the intercalation pocket, the phenanthroline part of the dppz ligand would be expected to be a severe steric hindrance for water hydrogen bonding to these aza nitrogens by this path. Thus, our data suggest that the aza nitrogens of the dppz ligand are rather close to the edge of the base pair that faces the Ru(II) ion. This notion is perfectly consistent with the suggestion by Barton et al.[41] that the Λ-enantiomer fits less well into the groove for an intercalative binding mode, since we observe that the luminescent lifetimes are on average 3.5 times longer for the Δ- compared to the Λ-enantiomers (Figure 4), which indicates that the phenazine nitrogens of Λ indeed are more accessible to water molecules.

However, our data suggest further that the base pairs in the floor and ceiling of the intercalation pocket are still shielding the phenazine nitrogens, since we find that the average ratio of comparable excited-state lifetimes for **1** vs **2** is 3.1 in poly-[dAdT]$_2$ compared to the average ratio 2.0 in polyol solvents, indicating that the direct steric hindrance by the 10-methyl group of solvent hydrogen bonding to one of the aza nitrogens of **1** is of greater importance in DNA than it is free in solution.

A very interesting observation is the surprisingly constant ratio of the short and the long lifetime in the DNA systems (Figure 3), suggesting the two lifetimes have similar structural origins in all six systems, origins that are thus not much perturbed by methyl substitution or Ru center chirality. Although it is premature to give a definitive answer to the question of the structural nature of the biexponential decays of Ru(II)-dppz complexes intercalated into DNA, we may rule out the possibility that the two lifetimes might have an origin in the sequential formation of hydrogen-bonded species, similar to the case in glycerol, since the magnitude of the (positive) α-values precludes that the long lifetime, which is associated with the less red shifted spectra and hence little hydrogen bonding, is an intermediate or precursor to the more red shifted species, associated with the short lifetime.

Conclusions

Methyl substituents on the distant benzene ring of the dppz ligand in [Ru(phen)$_2$dppz]$^{2+}$ strongly diminishes solvent hydrogen bonding to the excited state due to entropy, rather than enthalpy, factors. The observation that the solvent hydrogen bonding decreases both for the 10-methyl as well as for the 11,12-dimethyl derivative indicates that the effect is a steric perturbation of the whole solvent cage around the molecule. In contrast to the 11,12-dimethyl derivative, 10-methyl substitution decreases both the radiative and the nonradiative rate constant for decay to the ground state of the non-hydrogen-bonded excited-state species. The effects of methyl substitution is smaller when the complexes are intercalated into DNA, suggesting that the water molecules that quench the excited-state access the aza nitrogens of the dppz ligand from the groove where the Ru(II) ion resides. And, the almost constant ratio of the long relative to the short lifetime in all the 12 DNA systems suggests a structural origin to the two lifetimes that is practically invariant to methyl substitution or Ru center chirality.

Supporting Information Available: Differential absorption and LD spectra of **0**, **1**, and **2** bound to DNA. The absolute quantum yield as a function of *T* for **0**, **1**, and **2** in water. Steady-state emission spectra of the three complexes in polyol solvents and bound to DNA. Analysis and deconvolution of emission spectra with singular value decomposition. This material is available free of charge via the Internet at http://pubs.acs.org.

JA047166A